Arch. Hydrobiol.	113	3	405–424	Stuttgart, September 1988

The ultrastructure and physical characteristics of a distinctive colloidal iron particulate isolated from a small eutrophic lake

By Gary G. Leppard, J. Buffle, R. R. de Vitre and D. Perret

With 11 figures and 3 tables in the text

Abstract

An iron-rich fraction was isolated from a small eutrophic lake and studied on a particle-specific basis by transmission electron microscopy (TEM) in conjunction with energy dispersive spectroscopy. The limnological context from which the iron-rich fraction was isolated was characterized using a combination of in situ probes and analytical chemistry. An iron-rich colloidal particulate was identified; three morphotypes occurred, two of which could be described as globular and one of which as near-globular in shape. The size range determined by TEM was 0.05—0.31 μm, with three quarters falling in the narrow range of 0.05—0.13 μm. The latter range was found to be more representative of the true particle size distribution than a distribution found by filtration alone, which suggested an average particle size greater than 0.45 μm. Among the entire population of these colloids, ca. 70 % contained iron whereas most of the remaining 30 % were rich in either Si or Ca. Amongst the iron-rich globules, 86.5 % were also rich in phosphorus and calcium. Some evidence was found to suggest that Fe/P/Ca-rich particles were occasionally associated with either Si or Si/Al; however, the major fraction of these particles was found to contain exclusively Fe, P and Ca. These new findings are presented in the context of the limnological phenomena documented at the site.

Introduction

Iron plays an important role in aquatic ecosystems as a nutrient and as a modulator of the impact of other substances, such as bioavailable phosphorus and trace metals (Hutchinson, 1957; Wetzel, 1975). During the last two decades, a considerable amount of effort was put into understanding iron fluxes, as shown by the works of Verdouw & Dekkers (1980), Bloesch & Burns (1980), Davison et al. (1982), Liden (1983) and Davison (1985). A similar effort is being extended towards understanding redox transformations (Mayer et al., 1982; De Vitre, 1986) as well as towards gaining information on the morphology and chemical composition of lacustrine particulate iron (Giovanoli et al., 1980; Sholkovitz & Copland, 1982; Tipping et al., 1982; Liden, 1983). However, considering the growing body of evidence pertaining to the existence of colloidal-sized iron particles in natural aquatic systems, surprisingly few studies have combined STEM-EDS (scanning transmission electron micro-

0003-9136/88/0113-0405 $ 5.00

scopy in conjunction with energy dispersive spectroscopy) with classical limnological investigative approaches in order to obtain particle-specific data in the colloidal size range. The need to do so is particularly important since, in the colloidal size range (ca. 1—1000 nm), there are gaps in our understanding of the structure and physico-chemical transformations of naturally occurring amorphous iron. This paper is the first of a series addressing some of these gaps by providing:

1. characterizations on a particle-specific basis for lacustrine colloids rich in amorphous iron, by combining EDS with STEM;
2. technology transfer from the biomedical sciences to establish an optimal use of STEM in conjunction with high resolution TEM analyses of ultrathin sections of embedded colloid fractions;
3. an analysis of the new findings in the limnological context documented at the site.

Sampling and methods

Description of field site

Lake Bret is a small freshwater dimictic lake situated 10 km to the east of Lausanne, in the Canton of Vaud, Switzerland. Its principal hydrographic features are given in Fig. 1. The lake is used as a water reservoir and is characterized by a simple hydrology, namely one water inlet (the Grenet River) and one water outlet, a water treatment plant. Land use in the lake's extensive watershed is agricultural; this has led to heavy external phosphorus loading and to the lake's current hypereutrophic state. The summer season is characterized by the development of an extensive anoxic hypolimnion where high concentrations of reduced species of Fe, Mn, and S are found. The cycling and redox transformations of the latter species have been studied extensively (Zali, 1983; De Vitre, 1986; Buffle et al., 1987). However, no work has been reported previously on the chemical and physical nature of the particulate iron species found in the intermediate zone between the oxic surface waters and the anoxic hypolimnion. In Fig. 2 typical mid-summer concentration depth profiles for the particulate iron species, oxygen, orthophosphate and dissolved Fe(II) are given, along with a schematic representation of the interfacial zone between oxic surface waters and anoxic deeper ones. Both spatial and seasonal changes in the concentration of the particulate Fe species, other Fe species, Mn species, ortho-phosphate, calcium, O_2, sulfide, temperature and pH have been studied and are reported elsewhere (De Vitre, 1986; Buffle et al., 1988).

Sampling and analyses

Water samples containing the particulate iron species were obtained using a battery-driven peristaltic pump followed by sample isolation, as discussed below. All samples were obtained on 25 July, 1985, at a depth of 14 m, where a high concentration of the particulate Fe species is found (see Fig. 3). The water sample composition is given in Table 1. Dissolved O_2, temperature and pH were measured using an assembly of in situ probes (Orbisphere model 2112 for O_2 and temperature, linked to an Ingold model 503 for pH), whereas total and dissolved (smaller than 0.45 μm) Fe, Mn and Ca were determined by Flame Atomic Absorption on unfiltered and filtered samples respectively.

Lake Bret

Maximum length	1600 m
Maximum width	380 m
Maximum surface area	0.5 km^2
Maximum volume	4,565,000 m^3
Maximum depth	20 m
Altitude	673.5
Lake Watershed	2 km^2
Grenet Watershed	21.3 km^2
Mean residence time	1 year

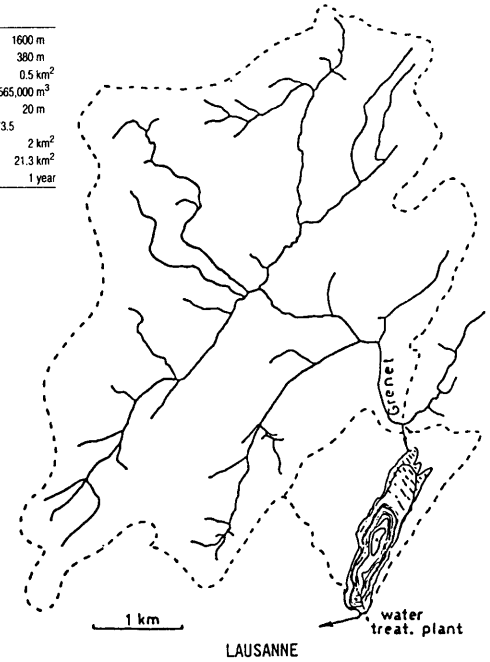

Fig. 1. Principal hydrographic and morphometric characteristics of Lake Bret, Vaud, Switzerland.

Fe(II) was also determined in both samples using the ortho-phenanthroline colorimetric procedure (APHA, Standard Methods, 1971). Differential Pulse Polarography was also done, using the methodology described by Davison et al. (1987), to determine the concentration of electroactive Mn(II) and Fe(II). Water samples for atomic absorption and colorimetry were collected in 10 ml polyethylene tubes and were acidified to pH = 2 with 1M HCl (Merck, pro analysi). Samples for polarographic measurements were stored in Winkler bottles in the dark and refrigerated at 8 °C (± 2 °C) until analysis. DPP was performed within 6 hr of sampling. Filtration was done using specially-designed plexiglass filter-holders and 90 mm diameter Schleicher and Schuell 0.45 μm filters. Filtration-based size distributions were also obtained using Plastipak B-D syringes equipped with Swin-lok filter-holders. In the latter case, 25 mm diameter Nuclepore filters with nominal pore sizes of 8, 5, 2 and 0.4 μm were used and approximately 40 ml of the water sample was filtered; this low volume allowed us to avoid clogging.

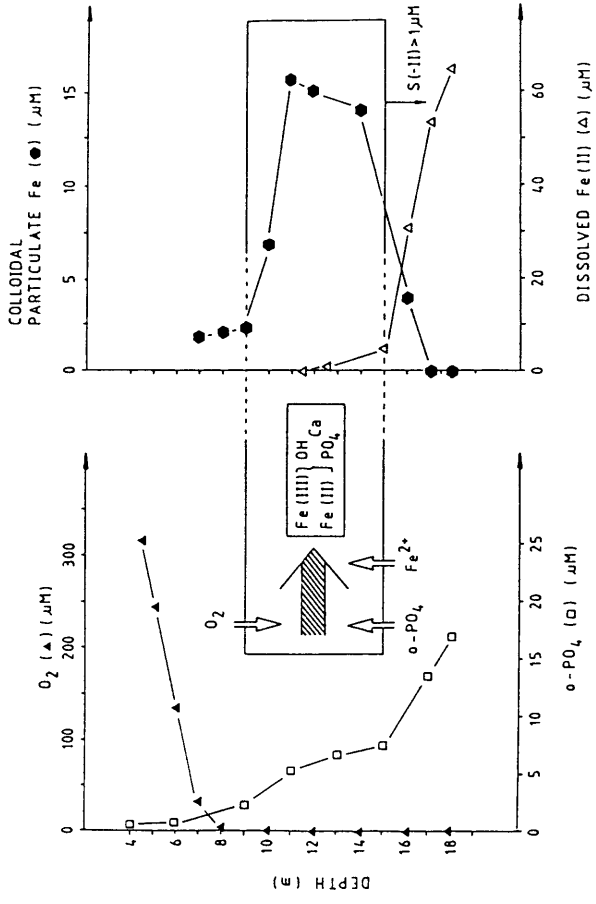

Fig. 2. Schematic representation of the in situ formation of the particulate colloidal-sized iron species in Lake Bret. The active zone is enclosed within a box, into which advective and diffusional transport of Fe^{2+}, o-PO_4^{3-}, and O_2 occurs leading to the formation of the colloidal particulate Fe phase whose main chemical components are shown enclosed in a box. Also shown are typical mid-summer depth concentration profiles for the above-mentioned species measured on 15 August, 1985.

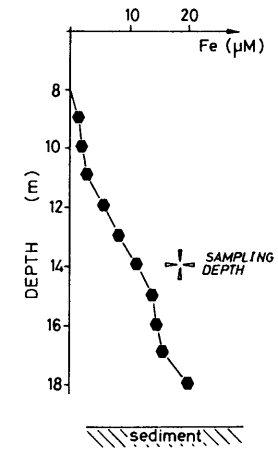

Fig. 3. Depth concentration profile of the colloidal particulate Fe species on 25 July, 1985.

Table 1. Physico-chemical parameters measured at the sampling site.

Dissolved O_2*		(mg/l)	0.1
Temperature*		(°C)	7.4
pH*			7.3
TOC*		(mg/l)	4.4
Alkalinity*[a]		(mM)	3.7
Ca^b	unfiltered	(mM)	1.4
	filtered	(mM)	n.d
$Fe_{tot}{}^b$	unfiltered	(μM)	9.6
	filtered	(μM)	0.5
Fe(II)[c]	unfiltered	(μM)	4.1
	filtered	(μM)	0.5
Fe(II)[d]	unfiltered	(μM)	0.2
$Mn_{tot}{}^b$	unfiltered	(μM)	6.8
	filtered	(μM)	6.8
Mn(II)[d]	unfiltered	(μM)	6.7

* unfiltered samples, [a] = determined by titration, [b] = determined by AAS, [c] = determined by colorimetry, [d] = determined by DPP, n.d. = not determined.

Sample preparation

In order to assess the importance of sample handling procedures and to prepare an "enriched" iron sample, two different sampling (filtration or centrifugation) and handling (untreated or freeze dried) procedures were tested (Fig. 4). Due to the delicately balanced redox environment within the zone from which the particles were isolated, as well as the very reactive nature (coagulation, adsorption, oxidation) of the iron particles studied, only simple physical separation methods are possible (De Vitre, 1986). All pre-

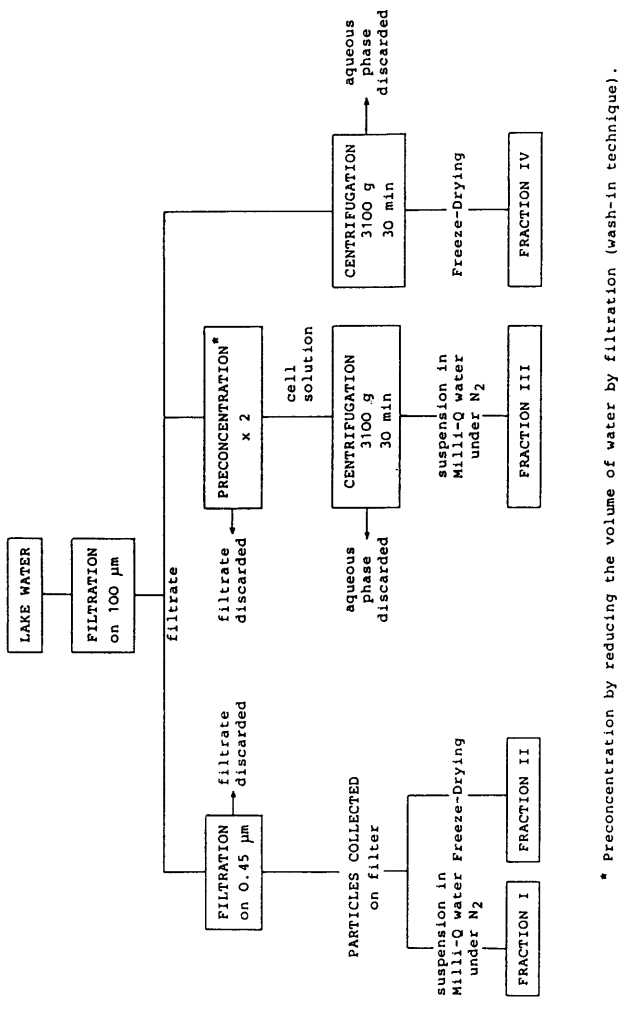

Fig. 4. Analytical separation scheme used to isolate and prepare iron-rich fractions for STEM-EDS.

parative separations were performed under an inert N_2 atmosphere and within 2 hr of sampling. Simple filtration was expected to yield a relatively unpurified sample, whereas centrifugation was expected to selectively isolate higher density particles (such as iron-rich particles) from lower density particles (such as organic-rich ones); these expectations were dependent on whether or not centrifugation introduced artifacts of coagulation, a phenomenon dealt with below. Both sample handling procedures were carried out to test possible effects (such as shrinkage and/or aggregation) of freeze-drying on the structure of iron-rich colloids and associated materials.

All samples were filtered initially through a 100 µm polyethylene filter to eliminate large particles (clay minerals, detritus, etc.). Fractions I and II were isolated by filtration through 0.45 µm filters. The particles were removed from the filter's surface under an N_2 atmosphere in a glove box and suspended in degassed Milli-Q water sterilized by filtration through a 0.2 µm filter (Fraction I) whereas Fraction II was freeze dried. Fractions III and IV were prepared by centrifugation (3100 g for 30 min) and were then treated in an analogous manner to Fractions I and II, yielding a wet and a freeze dried sample respectively. In the case of Fraction III, an additional pre-concentration step was included in order to increase the yield. All "wet" samples were subsequently stored frozen (the initial freezing being in liquid nitrogen); all samples which had been freeze dried were stored under a nitrogen atmosphere.

Analyses by conventional transmission electron microscopy

Preparation for conventional morphological analysis by TEM consisted of a sequential double chemical fixation (Burnison & Leppard, 1983) applied to each freeze dried fraction, followed by dehydration (solvent exchange) using a cold graded acetone series (20 % to 99.5 % at 4 °C) and then embedding in epoxy resin (Spurr, 1969) miscible with acetone. This preparatory procedure allows for a comparison of the lacustrine samples with known colloidal biologicals described in the literature on ultrastructure. Ultrathin sections (50—70 nm thickness) as estimated by the interference color method of Peachey (1958) were cut with a diamond knife, mounted in an LKB ultramicrotome (Ultrotome III), according to the systematic approach outlined in Leppard et al. (1977). Counterstaining of the sections, mounted on copper grids without a support film, was done according to Leppard et al. (1986). Observations and photographs were made with a Philips 300 TEM, operated at an accelerating voltage of 60 kV, on sections free of counterstain precipitate.

Two other procedures were employed to assess the conventional images in terms of potential artifacts which can result from (1) fixative-induced aggregation and (2) dehydration. Both were also utilized to improve the revelation of colloid infrastructure. The first of these, an acetone fixation procedure (Leppard et al., 1986), removes the influence of multivalent cations, buffer salts, oxidizing agents and cross-linking reagents used in conventional chemical fixatives: it also minimizes overstaining of aggregated particulates in the colloidal size range. This TEM preparatory procedure begins with the immersion of a freeze dried sample in acetone (99.5 %), then proceeding directly to the embedding step.

The final procedure consisted of embedding never-dried, never-fixed, never-stained, natural samples directly in a water-soluble melamine resin (Bachhuber & Frosch, 1983). The embedding medium selected was the medium-hardness formulation of the two-component resin system, Nanoplast FB 101, sold by J. B. EM Services, Inc., Pte. Claire, P. Q., Canada. We carried out the impregnation/hardening step in two stages: 2 days at 40 °C in a desiccator containing silica gel, followed by 2 days at 60 °C in a small

oven. The sectioning and photography were done as for the other two procedures above; counterstaining was found to be unnecessary.

Energy dispersive spectroscopy using STEM

A dual-stage scanning electron microscope (I. S. I. DS-130), equipped with a STEM attachment and an energy dispersive X-ray analyzer (γ-PGT/System 4), was used for all EDS analyses (CHANDLER, 1977). An accelerating voltage of 15 kV was applied to unstained sections (of 100—200 nm thickness) which were mounted on carbon coated, formvar covered, copper grids. The grid holder was tilted toward the detector from the horizontal at +10°, and 40 sec was selected as the counting time. Only obvious peaks (peaks more than double the height of the background signal) were considered in assessing the relative amounts of Fe in a given class of colloid. This latter rule was also applied to analyzing associations between Fe and the following elements: P, Ca, Si and Al. All analyses for specific elements were done on sections derived from the acetone fixation/epoxy embedding procedure. With this procedure, the native iron in the sectioned lacustrine materials provided sufficient electron opacity for visualizing the colloids most rich in iron. Silicon-rich structures were also readily visualized without the aid of any applied metal at any stage.

Results and discussion

General observations

Each principal iron-rich fraction (whether obtained by filtration or by centrifugation, whether processed as a freeze dried sample or as a wet sample) possessed certain general ultrastructural characteristics which were independent of the method of "cytological" preparation. These characteristics were:

1. the presence of many iron-rich colloidal particulates of roughly globular shape, the "globules" of Figs. 5 and 7, with diameters near 0.1 μm;
2. the presence of many identifiable biological structures (e.g., frustule fragments, tripartite membranes, fibrils, microbes) in the colloidal size range (Fig. 5);
3. great heterogeneity in the distribution of particulates (Fig. 5) which included many kinds of associations between iron-rich globules, identifiable biologicals and certain colloids tentatively identified as the physical units of organic-rich gels (e.g., the fibrils of Fig. 5 and the 2—3 nm granules of Fig. 6);
4. the apparent paradox that more than 90% of all particulates had least diameters much less than 0.45 μm, despite having been isolated originally on a filter of 0.45 μm pore size.

These four general characteristics suggest that lacustrine iron-rich particles cannot be assessed for their native size solely on the basis of filtration data. They also suggest that colloidal biologicals and organics may form more extensive associations with iron colloids than has been documented previously.

Fig. 5. An example of the great heterogeneity in the distribution of iron-rich particulates (in Fraction II) prepared for morphological analysis and counterstained according to BURNISON & LEPPARD (1983). Some globules are indicated by an arrow and a group of fibrils is indicated by a double arrow. The central portion of the micrograph is occupied by two microbial cells and their external capsules. The bar and subsequent bars represent 0.45 μm.

Morphology

The initial survey for identifiable and/or distinctive structures rich in native heavy metal revealed quite early the importance of electron-opaque globules and dense globule aggregates in a size range which ran from ca. 0.11 to ca. 2.5 times the pore size of the filter used to capture them. These proved to be extremely rich in Fe relative to other particles according to preliminary results from EDS. To correct for the aggregating and overstaining effects of the initial (cytological) fixative, the survey was redone using the acetone fixation procedure, with and without counterstaining. As a result, three morphological types of iron-rich globules were distinguished. These were:

1. simple globules with an indistinct interface between globule and external milieu (Fig. 7 A);

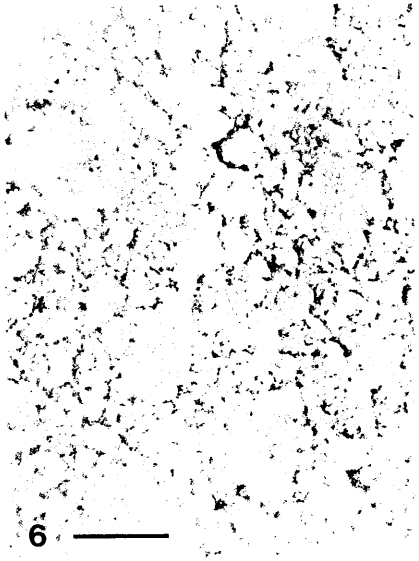

Fig. 6. Granules of 2—3 nm diameter aggregated into granule clusters which in turn are aggregated into a porous sponge-like network. Such relatively electron-transparent granules (after counterstaining) and their mode of aggregation following acetone fixation suggest the fulvic acid colloids of LEPPARD et al. (1986). Many of the largest clusters have a diameter in the range of 0.45—0.65 μm which are diameters of special interest to technologists involved in assessing water samples for particulate contaminants.

2. simple globules, as above, attached to and/or bearing a relatively large angular projection (identifiable in some cases as a fragment of diatom frustule — see arrow in Fig. 7 A);
3. globules with relatively small globulets projecting from an indistinct surface (Fig. 7 B).

Globules without globulets were common to all lacustrine preparations derived from freeze dried samples; globules with surface globulets were less common. In the case of simple globules attached to and/or bearing a large angular projection, preliminary spectroscopic analyses revealed that the strong iron peak was often accompanied by a strong silicon peak. With regard to the most simple globules, an inspection of many hundreds of views revealed no obvious differences in size between globules isolated by filtration alone and those isolated by centrifugation.

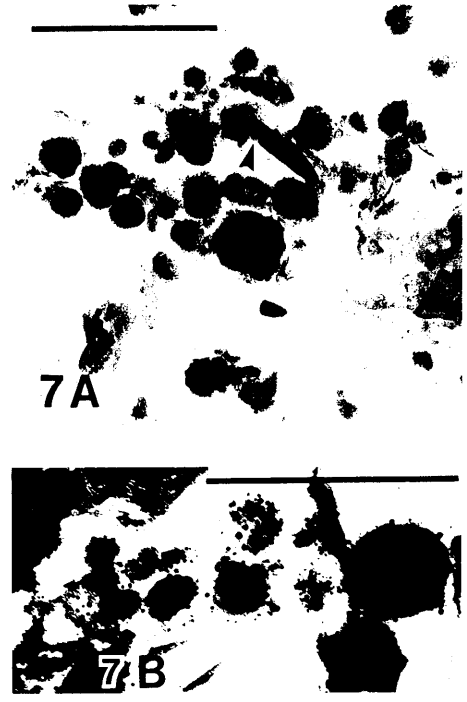

Fig. 7. Iron-rich, electron-opaque globules found in an iron-rich fraction isolated from Lake Bret. All heavy metal contributing to the electron opacity of this image was native heavy metal. (A) shows a cluster of simple globules (fixed in acetone) found in Fraction IV (centrifuged/freeze dried). Within this cluster, an arrow shows an extreme example of a globule with an angular projection. (B) shows globules bearing globulets (acetone fixation) found in Fraction II (filtered/freeze dried).

Size of iron particles — the role of sampling and handling

To assess shrinkage artifacts attributable to dehydration, the survey was repeated again using never-dried samples embedded directly in a hydrated Nanoplast mixture. The mixture of choice had a measured shrinkage during hardening of 2 % (see J. B. EM Services brochure on Nanoplast FB 101). The results showed no obvious size differences between individual globules prepared in Nanoplast and those prepared for sectioning via acetone fixation. Thus,

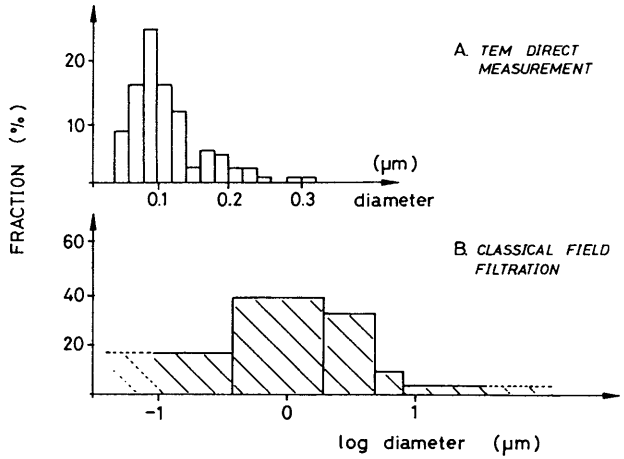

Fig. 8. Size distributions of the particulate Fe species found in the active zone (Fig. 2) of Lake Bret on 25 July, 1985. (A) shows a size distribution measured directly on micrographs obtained by TEM for particulates initially isolated by filtration on a 0.45 μm filter. (B) shows a size distribution obtained by direct field filtration, using syringes and Nuclepore filters.

shrinkage of globules can almost certainly be ruled out as the basis for the capture on a 0.45 μm filter of globules many times smaller.

Fig. 8 A illustrates graphically the results of pooling 122 separate diameter determinations. A comparison with Fig. 8 B makes clear the fact that globule diameter is not the major factor determining globule retention by filtration and that classical filtration conditions result in sizing data which are wrong by at least one order of magnitude (PERRET et al., 1987). The most common particle size determined by TEM was centred at 0.1 μm. Globules embedded in Nanoplast had a range of 0.053—0.307 μm, whereas those embedded in epoxy resin had a range of 0.048—0.238 μm. Among those in epoxy resin, globules isolated by filtration had a range of 0.064—0.172 μm, whereas those isolated by centrifugation had a range of 0.048—0.238 μm. The largest individual globules were found in Nanoplast sections and there were more exceptionally large globules in centrifugation isolates than in isolates derived by filtration. Thus, despite the similarity of size for typical globules in all preparations, there is some possibility that a much more extensive survey of globule diameters relative to type of preparation (tens of thousands of measurements) might produce some interesting new observations.

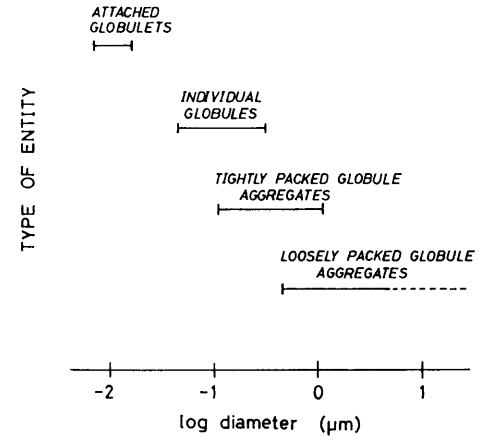

Fig. 9. Size classes of globules, globule aggregates and globule parts found in an iron-rich fraction originally isolated on a 450 nm filter.

Size of iron particles — sizing and morphological classification

Fig. 9 shows a size classification scheme relating globules, globule aggregates and globulets. Some 96 % of all globules were less than half the size of the pore of the collecting filter and some individuals were more than nine times smaller. It is likely that the loosely-packed aggregates have their final size and shape modified by sample processing and by interaction with the filter surface used to trap them (PERRET et al., 1987). For reasons described elsewhere (LEPPARD, 1984, 1985), an assessment of such modifications can be, at best, only partial and only semi-quantitative. Although the structure of such aggregates in the native (lacustrine) state was not pursued further, it was evident that associations between globules and other structures/materials could account for the apparently anomalous filtration behaviour of the globules. Much of the material of loosely-packed aggregates could be tentatively identified as biological and/or organic. Fibril aggregates of the type shown in Fig. 5 (LEPPARD, 1986) and granule aggregates of the type shown in Fig. 6 (LEPPARD et al., 1986) have been described as the principal component of some colloidal organic gels. Clearly, an iron-rich globule embedded in such a gel could result in a much larger sedimenting unit than indicated by a 48—307 nm least diameter; this larger unit could have a density much less than that of colloidal amorphous iron per se, a feature currently under examination. The most common particulate structures/materials found associated with iron-rich globules

Table 2. The most common particulates, as determined by TEM images, of epoxy embedded fractions.

I	Fine electron-opaque debris
	a) nondescript
	b) debris recognizable as cell parts (e.g., tripartite membranes, algal frustules, fibrils)
II	Microbiota (including pathological examples)
	a) prokaryotic cells
	b) eukaryotic cells
III	Clay leaflets
IV	Electron-opaque globular and near-globular structures (both simple and complex)
	a) with a strong iron signal
	b) without an iron signal
V	Fine granules of weak electron-opacity and diameter near resolution limit
	a) seen as a granule
	b) seen as a component of a dense aggregate

are categorized in Table 2. However, the exact nature of the association and its origin are subjects for future investigations.

Elemental composition

Electron-opaque globular colloids can be categorized by other than morphological criteria. Preliminary studies on more than one hundred such globules selected at random suggested that these colloidal sized particles could be classified according to their elemental composition. From the point of view of composition, four types of globules were delineated; they are listed in Table 3.

Within the category of type A iron-rich globules (Table 3), several distinct sub-categorizations can be made. The most frequently encountered elemental association was Fe/P/Ca; these three elements were present in 86.5% of all the

Table 3. Elemental composition-based groupings of electron-opaque globules. All EDS measurements (N = 127) were based on peak heights taken from colloids which received no heavy metal treatments of any kind.

Fraction of total globules (N = 127)		Fraction of Type A-globules (N = 89)	
Type	%	Type A	%
A – Iron-rich	70.1	– Fe/P/Ca	49.4
B – Si only	16.5	– Fe/P/Ca + Si/Al	22.5
C – Ca only	7.1	– Fe/P/Ca + Si	14.6
D – other(no Fe)	6.3	– other	13.5

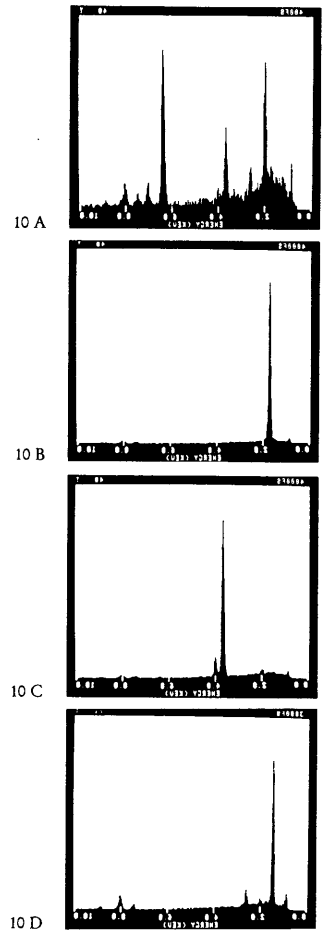

Fig. 10. Typical examples of EDS spectra for the four chemically different classes of globules isolated from Lake Bret waters.

iron-rich globules. However, within this latter group, 49.4% contained only these three elements while 22.5% also contained both Si and Al and 14.6% also contained only Si, thus suggesting that some of the iron-rich colloids

formed in the lake are associated with small clay fragments and/or silicon-rich particles such as frustule fragments. Note that a small subgroup (13.5 %) of the iron-rich particles had elemental associations which did not include both P and Ca. The data in Table 3 is based on 127 sets of spectral analyses and electron

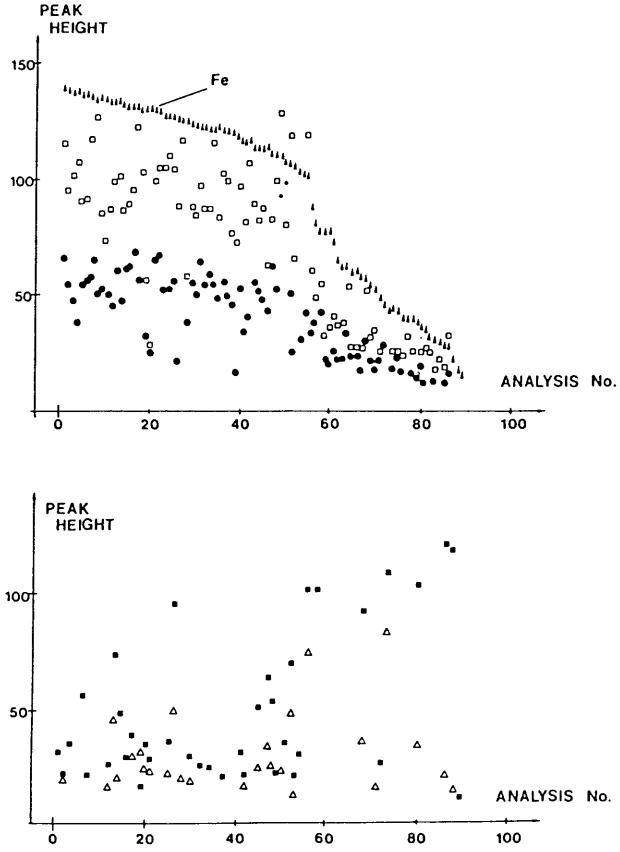

Fig. 11. Fe, P, Ca, Si, and Al peak heights recorded for 89 individual iron-rich globules (type A). Analyses are plotted arbitrarily as a function of decreasing iron content to facilitate visualization of possible correlations between the various elements. (▲ = Fe; □ = P; ● = Ca; ■ = Si; △ = Al).

micrographs and includes "near globules" to provide examples of colloids which are clearly hybrids of a globule and an angular particle.

Typical EDS spectra for the four chemically distinctive types of globular colloids are shown in Fig. 10. The principal Fe peak illustrated is the Kα peak which is centred about 6.4 keV, whereas Si, P, and Ca peaks occur at 1.7, 2.0, and 3.7 keV respectively. Shown in some spectra are two artifactual copper peaks (centred at 0.93 and 8.05 keV) which are generated by the copper support grid.

For EDS spectra of the quality shown in Fig. 10, the peak ratios (Fe/P, Fe/Ca, etc.) can be generally taken as an order of magnitude of molar ratios. Therefore, it can be informative to compare peak heights for the major elements (Fe, P, Ca, Si, and Al) of the 127 sets of spectra. This is shown in Fig. 11 where a clear correlation between Fe, P and Ca peak heights is shown. On the other hand, no obvious correlation between Fe and either Si or Al is apparent. These results will be discussed in detail elsewhere (Buffle et al., 1988). Note, however, that the average peak height ratios computed for the Fe/P/Ca particles (49.6 % of type A — see Table 3) are: Fe/P = 1.58 (σ = 0.38), Fe/Ca = 2.51 (σ = 0.48), and they ranged respectively from 0.85—2.48 and 1.06—3.8. Considering experimental error, the narrow ranges found for both the Fe/P and the Fe/Ca peak ratios strongly suggest constant particle composition. Furthermore, since the peak height ratio is within an order of magnitude of the molar ratio, it can be seen that the iron-rich particles contain a high proportion of both phosphorus and calcium.

Conclusions

Although the association of iron and phosphorus in naturally occurring iron oxyhydroxide is well known (Stumm & Morgan, 1981), no work to our knowledge has been published previously on Fe/P and Fe/Ca ratios determined on a particle-specific scale for amorphous iron colloids. The advantage of using a multielement microprobe technique linked to an electron microscope has been put to its full use and has enabled us to describe, both morphologically and chemically, some iron-rich colloidal particles found in the metalimnion of an eutrophic lake. Furthermore, when studying lacustrine oxyhydroxides of iron, filtration alone has been shown to be unsuitable in establishing a truly representative size distribution of the colloidal forms. We suggest that, when the necessary precautions are taken, TEM-based size distributions should be preferred. Further work investigating sizing is under way in order to clarify the apparently anomalous behaviour during filtration of the iron-rich colloids found in Lake Bret. Aggregation phenomena resulting from the interactions between such colloids and suspended organic matter are also being explored with the assistance of the novel technology of Bachhuber & Frosch (1983).

The new information that we have gained has enabled us to obtain a better understanding of the nature and the role of iron-rich colloids as a regulator of both iron and phosphorus dispersion in a lacustrine ecosystem. The technology of our research appears transferable to analyses of other naturally occurring colloids rich in heavy metals.

Résumé

Une fraction riche en fer a été isolée dans un petit lac eutrophe. Sa morphologie et sa composition chimique élémentaire ont été étudiées à l'aide d'un microscope électronique à transmission (TEM) équipé d'une microsonde EDS. Le contexte limnologique a été caractérisé en utilisant des sondes in situ ainsi que des méthodes analytiques classiques. Des particules de taille colloïdale, riches en fer, ont été mises en évidence; trois morphotypes dominants ont été observés, deux de forme globulaire et l'autre de forme quasi globulaire. Le diamètre des particules colloïdales, déterminé par TEM, était compris entre 0,05 et 0,31 μm. Dans 75 % des cas, ce diamètre était cependant compris dans une fourchette étroite de 0,05 à 0,13 μm. La distribution des tailles des colloïdes déterminée par TEM est plus représentative de la réalité que la distribution obtenue par filtration (suggérant un diamètre moyen supérieur à 0,45 μm). Environ 70 % de la population totale des particules colloïdales est riche en fer; les 30 % restants sont riches soit en silicium, soit en calcium. Parmi les globules riches en fer, 86,5 % sont également riches en phosphore et en calcium. Les particules riches en Fe, P et Ca contiennent parfois du silicium et parfois du silicium et de l'aluminium; toutefois, la majeure partie de ces particules contient exclusivement Fe, P et Ca. Ces nouveaux résultats sont discutés dans le contexte des phénomènes limnologiques étudiés sur le site.

Acknowledgements

We thank Ms. J. Carson and Dr. J. Lott of McMaster University, Hamilton, Canada, for their assistance with electron microscopical facilities. We thank also Dr. D. Frosch of the University of Ulm, West Germany, for technical advice. This work was partly supported by the Swiss National Foundation (Project 2.310-0.84).

References

APHA (1971): Standard methods for the examination of water and wastewater, 13th edition. — Amer. Public Health Assoc., Washington, D. C. 1—874.

Bachhuber, K. & Frosch, D. (1983): Melamine resins, a new class of water-soluble embedding media for electron microscopy. — J. Microsc. **130:** 1—9.

Bloesch, J. & Burns, N. M. (1980): A critical review of sedimentation trap technique. — Schweiz. Z. Hydrol. **42:** 15—55.

Buffle, J., Zali, O., Zumstein, J. & De Vitre, R. (1987): Analytical methods for the direct determination of inorganic and organic species: seasonal changes of iron, sulfur and pedogenic and aquogenic organic constituents in the eutrophic Lake Bret, Switzerland. — The Science of the Total Environment **64:** 41—59.

Buffle, J., De Vitre, R. R., Perret, D. & Leppard, G. G. (1988): Physicochemical characteristics of a colloidal iron phosphate species formed at the oxic-anoxic interface of an eutrophic lake. — Geochim. Cosmochim. Acta (accepted).

Burnison, B. K. & Leppard, G. G. (1983): Isolation of colloidal fibrils from lake water by physical separation techniques. — Can. J. Fish. Aquat. Sci. **40:** 373—381.

Chandler, J. A. (1977): X-ray microanalysis in the electron microscope. — North-Holland Publ. Corp., Amsterdam. 317—547.

Davison, W. (1985): Conceptual models for transport at a redox boundary, pp. 31—53. — In: Stumm, W. (ed.) Chemical processes in lakes. — Wiley-Interscience, New York.

Davison, W., Buffle, J. & De Vitre, R. (1987): Voltammetric measurements of aquatic species without sample modifications: Recommendations for the determination of O_2, Fe(II), Mn(II), S(−II) and related species in anoxic waters. — Pure and Applied Chemistry, IUPAC (in press).

Davison, W., Woof, C. & Rigg, E. (1982): The dynamics of iron and manganese in a seasonally anoxic freshwater lake: Direct measurement of fluxes using sediment traps. — Limnol. Oceanogr. **27:** 987—1003.

De Vitre, R. (1986): Multimethod characterization of the forms of iron, manganese and sulfur in a eutrophic lake (Bret, Vaud, Switzerland). — Ph. D. Thesis, University of Geneva. No. 2224.

Giovanoli, R., Brutsch, R., Diem, D., Osman-Sigg, G. & Sigg, L. (1980): The composition of settling particles in Lake Zürich. — Schweiz. Z. Hydrol. **42:** 89—100.

Hutchinson, G. E. (1957): A treatise on limnology, Vol. 1. — Wiley & Sons, New York. 1—1015.

Leppard, G. G. (1984): The ultrastructure of lacustrine sedimenting materials in the colloidal size range. — Arch. Hydrobiol. **101:** 521—530.

— (1985): Transmission electron microscopy applied to water fractionation studies — A new look at DOC. — Wat. Pollut. Res. J. Can. **20** (2): 100—110.

— (1986): The fibrillar matrix component of lacustrine biofilms. — Wat. Res. **20:** 697—702.

Leppard, G. G., Buffle, J. & Baudat, R. (1986): A description of the aggregation properties of aquatic pedogenic fulvic acids — Combining physico-chemical data and microscopical observations. — Wat. Res. **20:** 185—196.

Leppard, G. G., Massalski, A. & Lean, D. R. S. (1977): Electron-opaque microscopic fibrils in lakes: their demonstration, their biological derivation and their potential significance in the redistribution of cations. — Protoplasma **92:** 289—309.

Liden, J. (1983): Equilibrium approaches to natural water systems — Part 3. — Schweiz. Z. Hydrol. **45:** 411—429.

Mayer, L. M., Liotta, F. P. & Norton, S. A. (1982): Hypolimnetic redox and phosphorus cycling in hypereutrophic Lake Sebasticook, Maine. — Wat. Res. **16:** 1189—1196.

Peachey, L. D. (1958): Thin sections — 1. A study of section thickness and physical distortion produced during microtomy. — J. Biophys. Biochem. Cytol. **4:** 233—242.

Perret, D., De Vitre, R., Leppard, G. G. & Buffle, J. (1987): unpublished results.

Sholkovitz, E. R. & Copland, D. (1982): The chemistry of suspended matter in Esthwaite Water, a biologically productive lake with seasonally anoxic hypolimnion. — Geochim. Cosmochim. Acta **46:** 393—410.

Spurr, A. R. (1969): A low-viscosity epoxy resin embedding medium for electron microscopy. — J. Ultrastruct. Res. **26:** 31—43.

Stumm, W. & Morgan, J. J. (1981): Aquatic chemistry, 2nd edition. — Wiley-Interscience, New York. 1—780.

Tipping, E., Woof, C. & Ohnstad, M. (1982): Forms of iron in the oxygenated waters of Esthwaite Water, U. K. — Hydrobiologia **92:** 383—393.

VERDOUW, H. & DEKKERS, E. M. J. (1980): Iron and manganese in Lake Vechten (The Netherlands); dynamics and role in the cycle of reducing power. — Arch. Hydrobiol. **89**: 509—532.

WETZEL, R. G. (1975): Limnology. — W. B. Saunders, Philadelphia. 1—743.

ZALI, O. (1983): Cycles chimiques dans un lac eutrophe, en particulier espèces du Fe, Mn, S et P dans le lac de Bret. — Ph. D. Thesis. University of Geneva. No. 2090.

Addresses of the authors:

GARY G. LEPPARD, National Water Research Institute, Burlington, Ontario L7R 4A6, Canada.

J. BUFFLE, R. R. DE VITRE, and D. PERRET, Département de Chimie Minérale, Analytique et Appliquée, Université de Genève, 1211 Genève 4, Switzerland.